Drive of feed axes of NC machines with 2 motors

Ing. Vojtěch Matyska

Vedoucí: Doc. Ing. Pavel Souček, DrSc.

Abstrakt

Hlavními požadavky kladenými na pohybové osy NC obráběcích strojů jsou vysoká přesnost polohování a vysoká dynamika pohybů. Základní předpoklad pro dosažení těchto protichůdných předpokladů je však tuhá a lehká konstrukce mechanické struktury stroje. Těmito parametry je dána výše první antirezonanční frekvence, která omezuje nastavení zesílení kaskádně uspořádaných regulátorů rychlosti a polohy. Nastavení těchto zesílení je také ovlivněno druhem použitého pohonu a jeho uspořádání. Příspěvek se zabývá vlivem použití dvou synchronních motorů v pohonu posuvové osy NC stroje a jejich paralelního řízení se společným odměřováním polohy na celkové dynamické chování stroje a následně na nastavení regulace.

Klíčová slova

Přímé odměřování, antirezonanční frekvence, kaskádní regulace.

1. Introduction

The main demands placed on NC machine tools feed drive axis are high precision positioning and high dynamics. Important prerequisites for achieving these contradictory requirements are stiff and lightweight design of feed drive axis. These parameters determine the value of the first antiresonant frequency, which limits the gain settings of cascade arranged regulators of speed and position. The settings of these gains are also influenced by a type of used drive and its structure. The contribution focuses on the influence of the usage of 2 permanent magnet synchronous motors (PMSM) – sometimes called electrically commutated or brushless synchronous motors – in NC machine linear feed drive axis and theirs parallel control with joined measurement of position end to overall dynamical behaviour of NC machine and its regulation settings.

Today, two PMSMs are commonly used in lot of NC machine tools, manipulators and so on because of a lot of various reasons. One of these reasons is to provide functionality when a failure occurs. This is crucial especially in aeronautics, where a lot of hydraulic systems (which are always doubled, tripled or even quadrupled) have been removed with electric motors (also at least doubled) or in manipulation with dangerous (nuclear) materials. Another reason for the usage of 2 PMSMs is to compensate flexibility of long movable parts of machine tools like gantries (example in figure 1). If the gantry was driven with only one PMSM, it would become so deformed that it would lose its precision or even get jammed. And these PMSMs are often driven with cascade regulation in the gantry form. There are a lot of papers that focus on modifications of regulators to improve the precision of a machine, mostly for assembling electrical circuits.

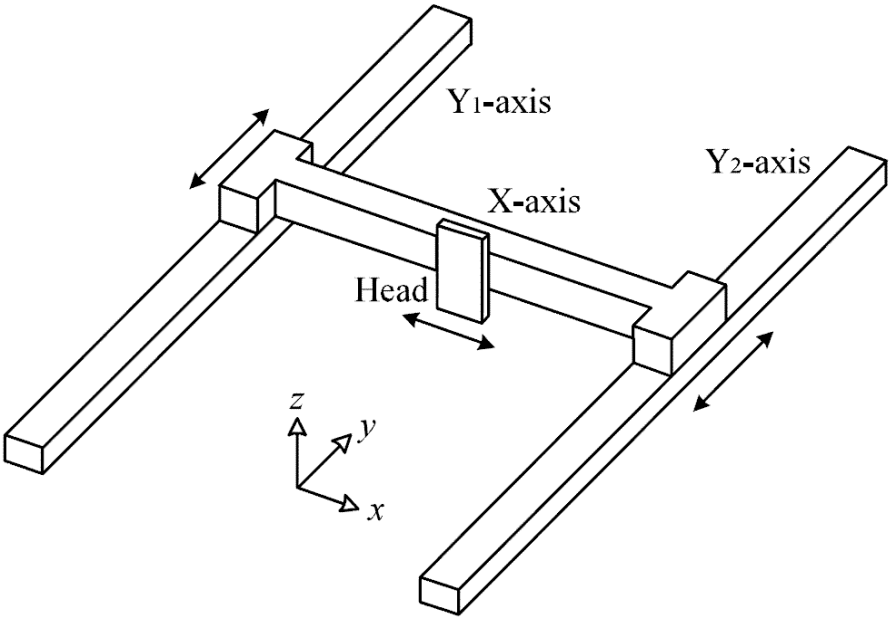

Fig. 1: *Schema of gantry machine tool [4]*

In these examples (also presented in [1] through [4]) two PMSMs are connected to one ball screw each or two linear motors are used, but both PMSMs are never connected to one ball screw, one on each side of screw. Today only one PMSM is commonly used for one screw. There is a Japanese patent [5] which describes the usage of 2 PMSMs on one ball screw, moreover with direct encoding. This patent focuses mainly on reduction of moment of inertia of motors and screw assembly which increases the maximal acceleration of a feed axis. It also shows that you could use the longer screw without a loss of accuracy because the deformation of one long screw part is compensated by the other motor on the shorter part. But this patent mentions no effect to eigen modes and frequencies, as described later in this paper. Lately, the first time at exhibition EMO 2009 in Milano, new principles of driving feed axes have been used in real machine tool. These principles are showed in [6]. FANUC presented 3 conceptions with 2 PMSMs (figure 2). These conceptions use either an independent regulation with only one required and actual (measured) position (direct encoding) – rotary table and spindle – or an independent regulation of both motors like common gantries (indirect encoding) with compensation of a speed interference – lathe. 2 PMSMs in lathe are used for compensating of long work-piece deformation, in the table and spindle for reducing the moment of inertia (the same as in [5]) and for preloading of the transmission between the motor and the table (spindle).

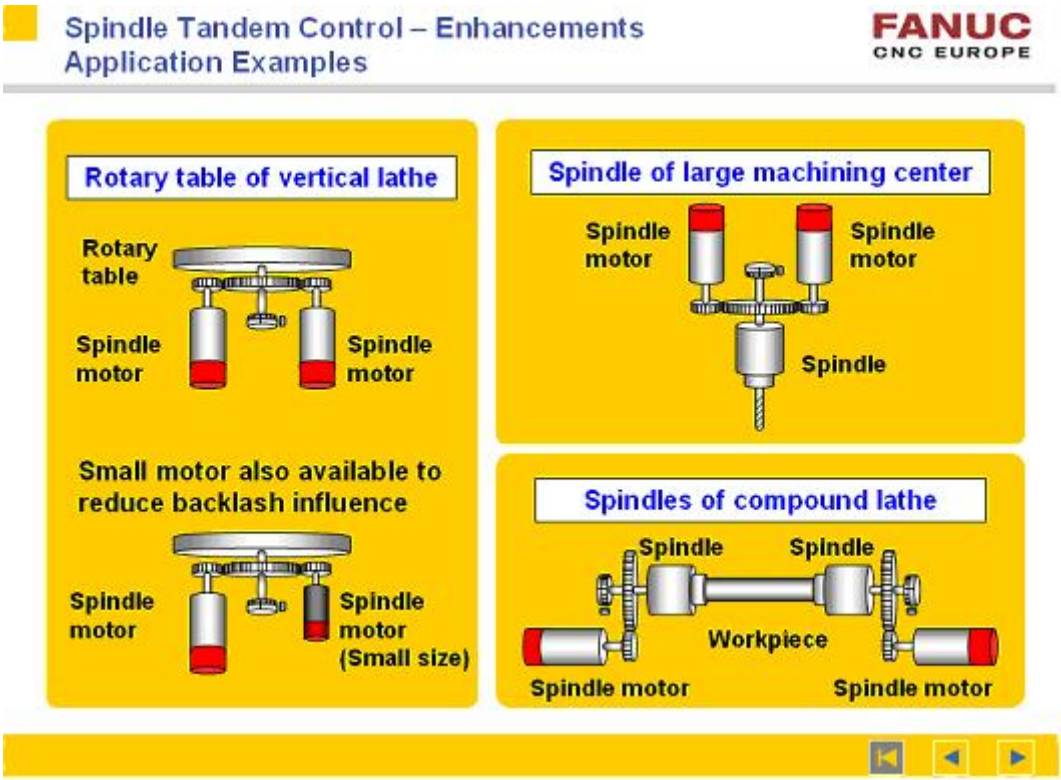

Fig. 2: *Conceptions with 2 PMSMs by FANUC [6]*

Another example of the usage of 2 PMSMs (this time on a single ball screw) shown at EMO 2009 exhibition is a machine tool by MCM (figure 3). M1 and M2 in the figure stand for motors.

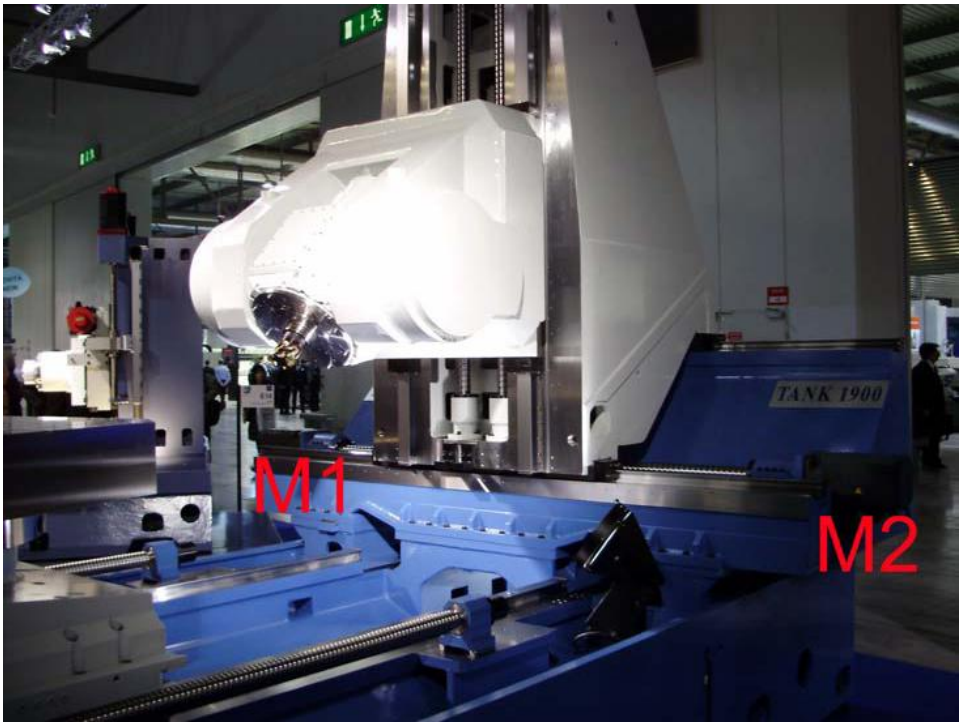

Fig. 3: *Machine tool with 2 PMSMs by MCM [6]*

2. Principle of synchronous regulation

The principle and advantages of the usage of 2 PMSMs in feed axes (where only one is commonly used) are described in [6]. The paper includes calculations in terms of dynamical system shown in the figure 4 and 5.

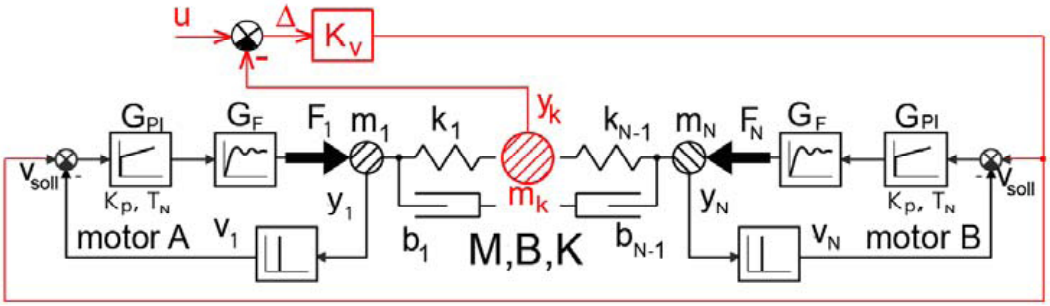

Fig. 4: *Dynamical model of regulation and mechanics of feed axis [6]*

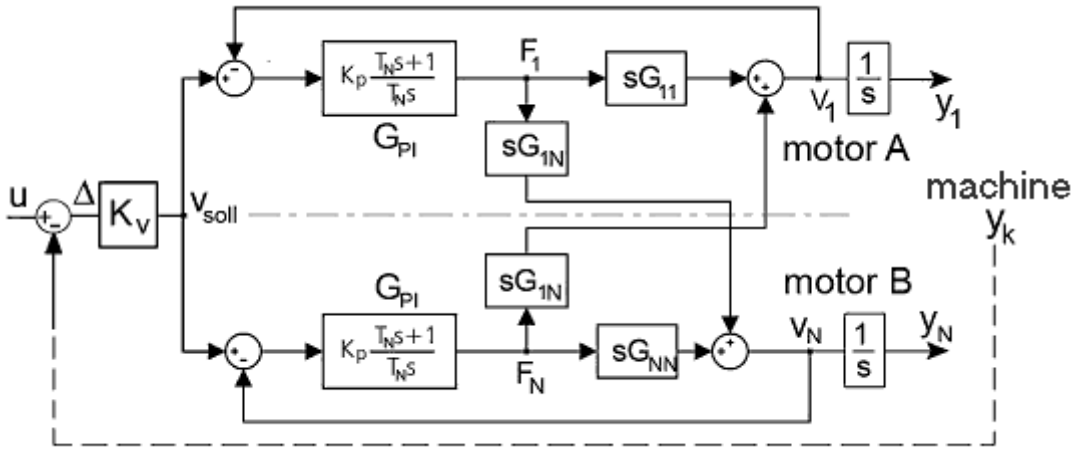

Fig. 5: *Block diagram of synchronous position control [6]*

In these figures G_{PI} stands for the velocity regulator transfer function, $G_F = 1$ for the well calibrated current regulator transfer function, K_V for a proportional gain of position regulator, y_i for the position, v_{soll} for the desired speed, s for the parameter of Laplace transform (it can be substituted $s = j\omega$) and $G_{ij} = G_{ji}$ for the transfer function of mechanics from force (torque) on mass i to position of mass j (and vice versa). Transfer functions $G_{ij} = G_{ji}$ are expressed from matrices M (mass), B (friction) and K (rigidity). This expression is shown in equations (1) through (3). In the figures it is also shown that the actual position is measured from inner part of the machine (e. g. a table) – direct encoding is used.

$$M \cdot \ddot{y}(t) + B \cdot \dot{y}(t) + K \cdot y(t) = f(t) \tag{1}$$

$$y(t) = (s^2 \cdot M + s \cdot B + K)^{-1} \cdot f(s) = G(s) \cdot f(s) \tag{2}$$

$$G(s) = \begin{bmatrix} G_{11}(s) & G_{12}(s) & \cdots & G_{1N}(s) \\ G_{21}(s) & G_{22}(s) & & G_{2N}(s) \\ \vdots & & \ddots & \vdots \\ G_{N1}(s) & G_{N2}(s) & \cdots & G_{NN}(s) \end{bmatrix} \tag{3}$$

The equation (2) is expressed from (1) using Laplace transform and the symmetrical matrix $G(s)$ of transfer functions is described in (3).

Based on analytical calculations in [6] (performed for 3-mass system – the system was used for its simplicity) it was discovered that this type of the drive of feed axis has a significant influence on its dynamical properties. For example, some eigen modes are suppressed and some antiresonance frequencies are shifted. This was also confirmed by simulations (which I had done myself) in Matlab/Simulink environment and an experiment conducted on a small testing bed. The testing bed consists of discs on a thin beam (which serves as torsion springs) with 2 PMSMs and it is shown on the figure 6.

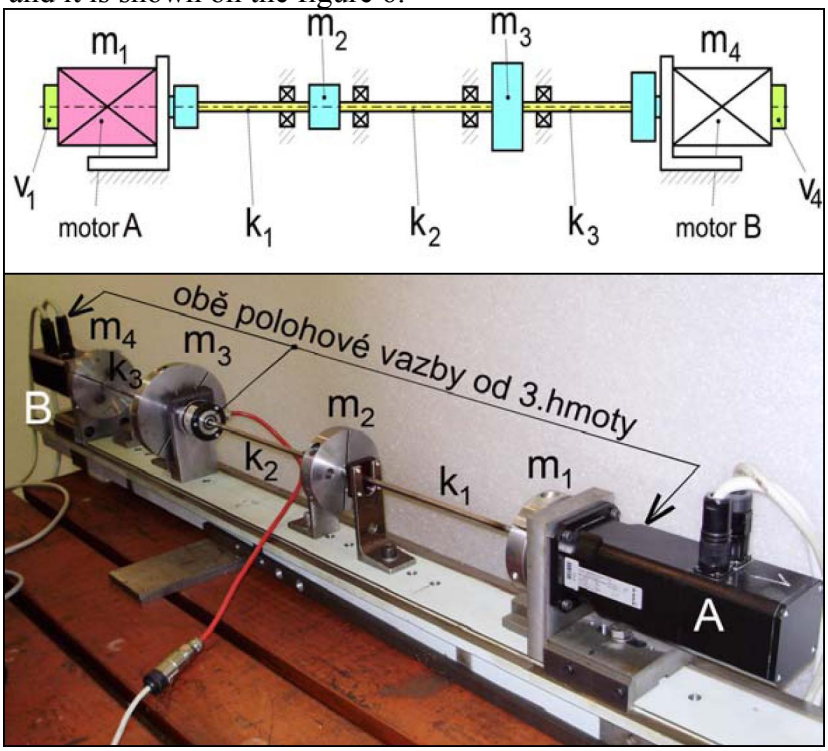

Fig. 6: *Schema and photo of 4-mass testing bed [6]*

As stated above, position control obtains the actual position from an encoder connected to the mass m_3 (direct encoding). Results of both simulations and experiments matched (Due to the simplicity of the testing bed. There were very few parameters that could cause differences.) and confirmed the conclusions of the calculations mentioned above. Some of the results are shown in the figures 7 and 8. In the figure 7 the left graph shows results of the simulation with only motor A used. The right graph shows results of the simulation with both motors A and B used. In the figure 8 these results are compared. In both figures the blue curve stands for the transfer function $s \cdot G_{11}(\omega) = \frac{\dot{\varphi}_1(\omega)}{M_{k1}(\omega)}$ (only one PMSM used – motor A) and the green curve for the transfer function $\frac{\dot{\varphi}_1(\omega)}{M_{k1}(\omega)+M_{k4}(\omega)}$ (both PMSMs used – motor A and B). In the figure 7 the red curves stand for transfer functions of the velocity control $\frac{\dot{\varphi}_{1akt}(\omega)}{\dot{\varphi}_{1soll}(\omega)}$ in both cases of measurement conditions.

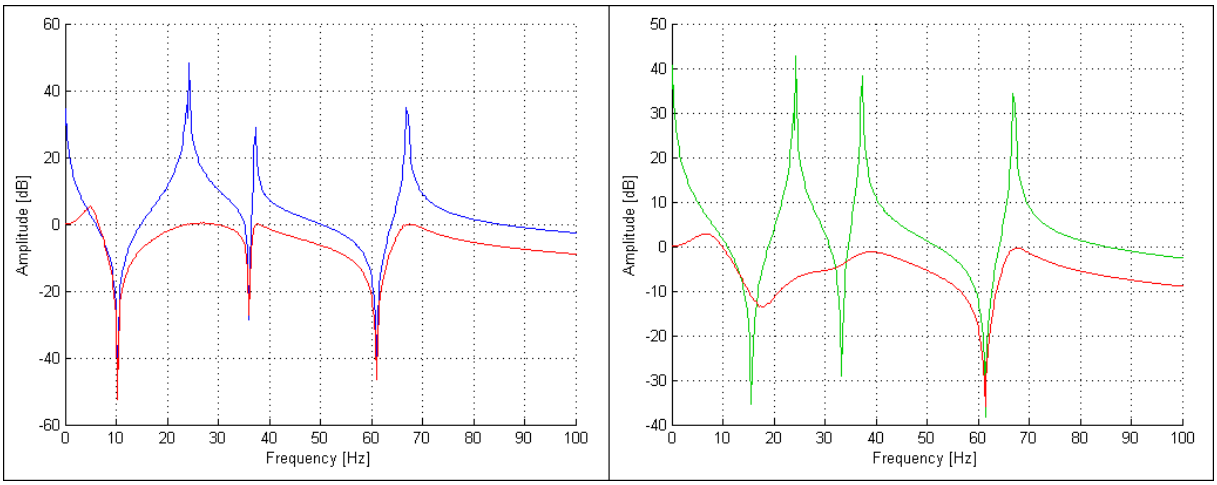

Fig. 7: *Transfer functions – one PMSM and 2 PMSMs*

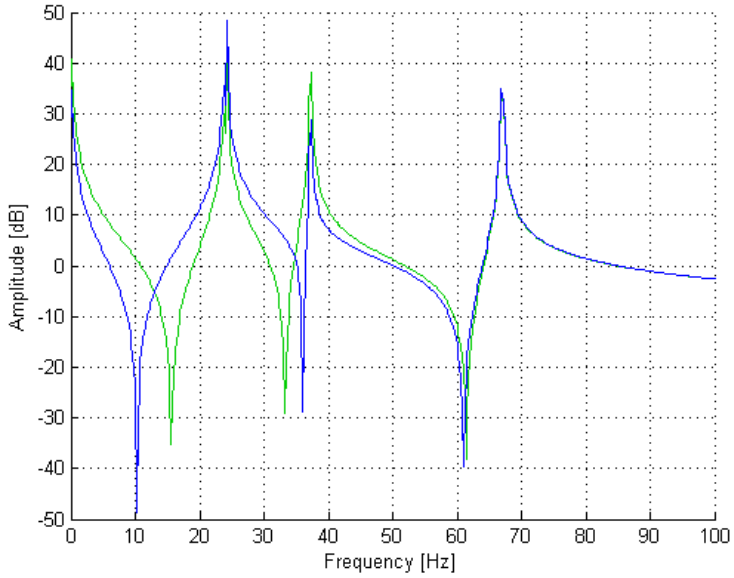

Fig. 8: *Transfer functions – comparison of one PMSM and 2 PMSMs*

There is a very apparent effect of the usage of both PMSMs in the suppression of the second antiresonance frequency (caused by the suppression of the third eigen mode; it is well known that the velocity control suppresses resonant peaks of transfer functions). Also the second eigen mode is partially suppressed. In the figure 8 shifts of antiresonance frequencies caused by the usage of 2 PMSMs are shown.

These effects on the dynamical behaviour of the mechanical system can be used for adjusting parameters of speed and position control, as shows table 1.

Table 1. *– Parameters of speed and position control.*

	One PMSM (motor A)	**Both PMSMs**
$K_P\ [A \cdot s \cdot rad^{-1}]$	0.4	0.4
$T_N\ [s]$	0.12	0.06
$K_V\ [s^{-1}]$ – optimal	15 ÷17	45 ÷46
$K_V\ [s^{-1}]$ – stability limit	approx. 80	approx. 125

3. Preparation of testing bed

The simplicity of the computations, models and experiments outlined above has some advantages but also some disadvantages. The advantages are that due to the simplicity, the computations can be made analytically (and even by hand), which means that many rules and trends can be derived and predicted, 4-mass testing bed could be easily constructed and experiments and simulations are likely to have the same results. The main disadvantage is that the 4-mass testing bed and a real machine tool are quite different so many people are not convinced that this principle can work on a real machine. That is probably the main reason why this kind of drives is so rare even though the influence of the usage of 2 PMSMs has such a significant effect on regulation parameters (table 1).

Consequently my first task was to build a testing bed much more similar to a real machine tool, where 2 PMSMs will be used on one ball screw so that the advantages could be clearly seen. I decided to use and modify a testing bed STD-3 because it has one feed axis with parts such as linear guides and a sliding table which can be used for the measuring. The bed itself was made from an old machine bed of grinding machine, therefore the similarity to the real machine tool is apparent. The effect of the usage of 2 PMSMs could be demonstrated more easily on a long ball screw that had to be ordered. The length of the screw was designed up to ca 2000 mm with respect to critical rotation speed and buckling stress. Beside the length, the chosen diameter of 32 mm makes the screw very flexible, so the results of the experiment should be very convincing. Another part of the modified STD-3 represents a machine column with a tool holder and it is part of testing C-frame that had been made for experiments with heat deformations. The design of the modified STD-3 is shown in the figure 9.

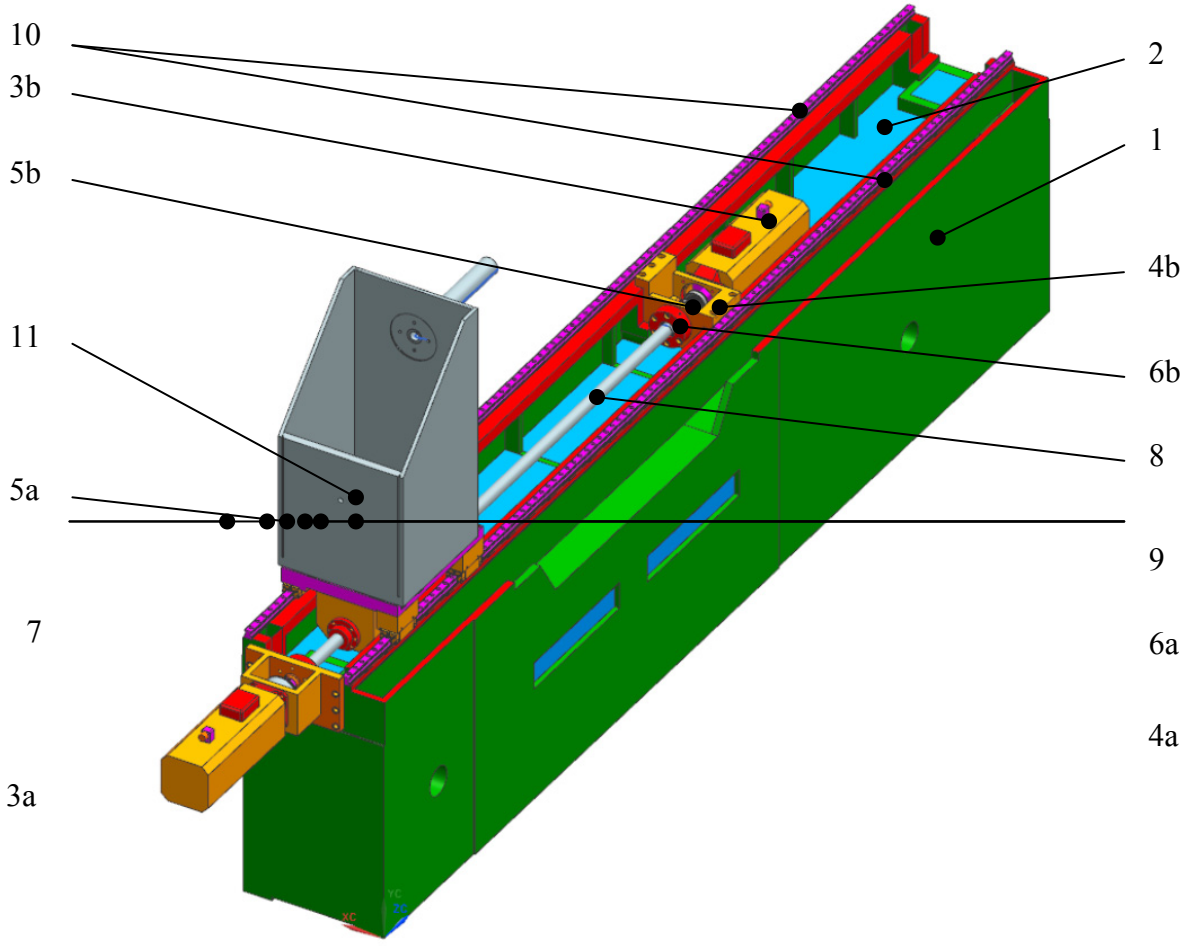

Fig. 9: *CAD model of STD-3*

The modified testing bed STD-3 is based on the machine bed 1. There is the sand filling 2 inserted into the bed to increase structural damping. Two identical servomotors 3a and 3b are attached to the bed using motor holders 4a and 4b. There are the couplings 5a and 5b tightened on the motor shafts to transfer the torque to the ball screw 8. Each end of the screw is mounted to the motor holder with bearing housings 6a and 6b. There is the axial-radial bearing in housing 6a and radial bearing in housing 6b which allows an axial deviation of this end of the screw. The additional weight 7 can be attached to the coupling 5a. The ball screw moves the sliding table 9 with the connected ball nut. The sliding table moves along the linear guides 10 and holds the column 11. The column includes the rod to simulate a tool holder and it can be turned by 90 degrees around vertical axis to test another position.
To simulate driving with only one motor, the coupling 5b will be disconnected from the screw and the additional weight 7 will be attached to the coupling 5a to simulate the servomotor with double moment of inertia. To simulate driving with both motors, the coupling 5b will be connected, additional weight removed and maximal torque of each motor will be limited to one half (as the simulation of two weaker motors).

4. Research work

The modified testing bed STD-3 is ready to assemble, but this can't be done at the moment because it is being used for some other experiments and teaching. STD-3 is in its original form (only one PMSM 3a, a shorter ball screw and no column on the sliding table), but because a lot of parts are going to remain the same in its modified version, some preparations and measurements have been done. The aim of these preparations is to verify the parameters of the prepared FEM model of STD-3. This verification is important because some parameters (as modulus of elasticity of the sand filing) aren't stated in catalogues (they must be measured separately). Some parameters which are stated in catalogues (as ball nut axial stiffness) are very inaccurate – they can differ by 50 through 70 percent. These variations can be caused by the difference between laboratory conditions (when measured by producers of the parts) and real conditions (when used in machine tools). In order to execute this verification FEM model of the original STD-3 was made (derived from already complete FEM model of modified STD-3) and some measurements were performed on this testing bed. Both measurements and FEM calculations were made with several types of couplings, with two weights of the sliding table and in different positions of the sliding table in order to get more data with greater variety so that these uncertain parameters could be determined with smaller deviation.
To illustrate how an incorrect parameter can change the results, the figure 10 shows transfer functions of speed control $\frac{\dot{\varphi}_{1akt}(\omega)}{\dot{\varphi}_{1soll}(\omega)}$ used on 2 FEM models – one with incorrect stiffness of rubber spring insulator (which the testing bed lies on) and one with the correct (verified) one. The blue curve in the figure 10 represents incorrect stiffness, the red curve represents the correct one. The first antiresonant drops (about 53 Hz in the blue transfer function and about 7.5 Hz in the red one) belong to the vibration of the whole testing bed on rubber insulators and the difference is apparent. The incorrect stiffness also changes frequencies of other eigen modes of the testing bed. A similar example of the influence of the accuracy of these parameters (not shown) is torsion stiffness of the one used couplings. Producer's catalogue shows stiffness 9000 Nm/rad but the measured and verified value is only 3200 Nm/rad. This value was obtained by comparing measured and calculated transfer functions. By this procedure many other parameters (other stiffnesses of couplings, ball nut stiffness, modulus of elasticity of sand filing and damping of particular eigen modes connected with bending of bed and with rubber insulators) were also verified. Also model of the connection between the

bed and the motor holder was modified to be more accurate. Some other comparisons of transfer functions are shown in figures 11 through 14 and described below.

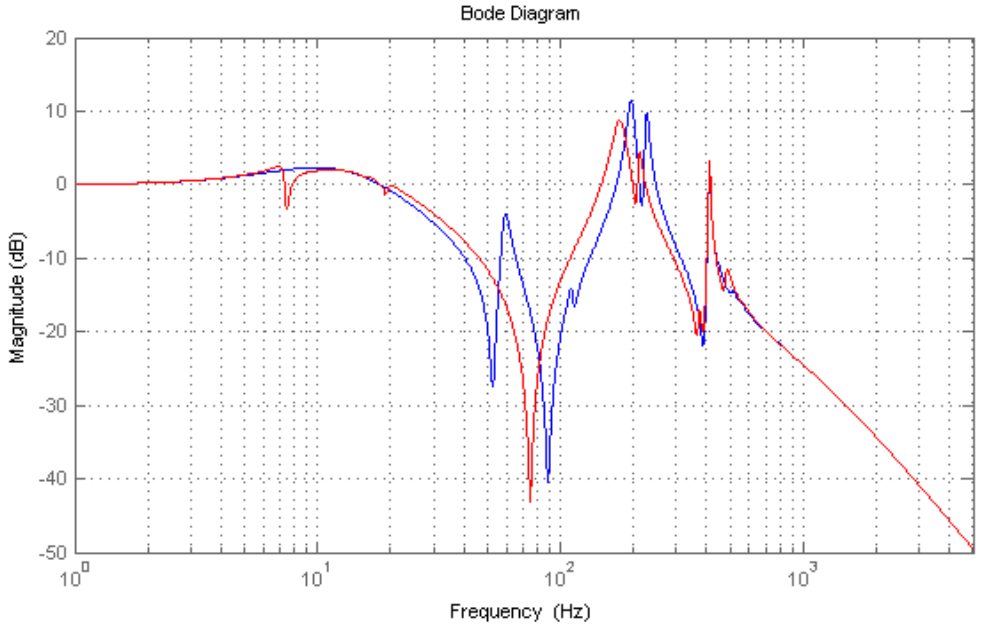

Fig. 10: *Transfer functions – comparison of incorrect stiffness of rubber spring insulator and the correct one (coupling MAYR SMARTFLEX used, table near PMSM)*

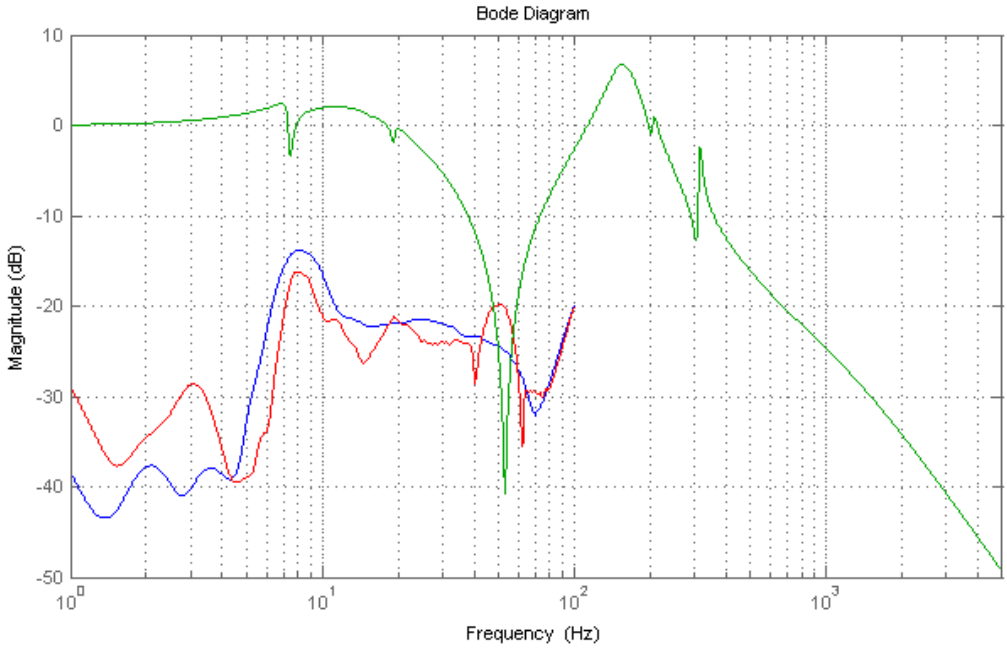

Fig. 11: *Transfer functions – verification of stiffness of rubber insulator (coupling MAYR ROBA ES used)*

There are 3 transfer functions in the figure 11. The blue and red one show links between the torque of PMSM and acceleration of the whole bed. These were measured with an accelerometer in different table positions and the resonance around 8 Hz belongs to the bed vibration on rubber insulators. It is apparent that the position of the table doesn't influence the eigen mode much. The differences are probably caused by the measurement inaccuracy (measurements in low frequencies are always inaccurate). The green curve shows a transfer function of speed control without damping applied and correct stiffness is used. The first

antiresonant drop (about 7.5 Hz) belongs to the same eigen mode and its frequency corresponds to the measurement.

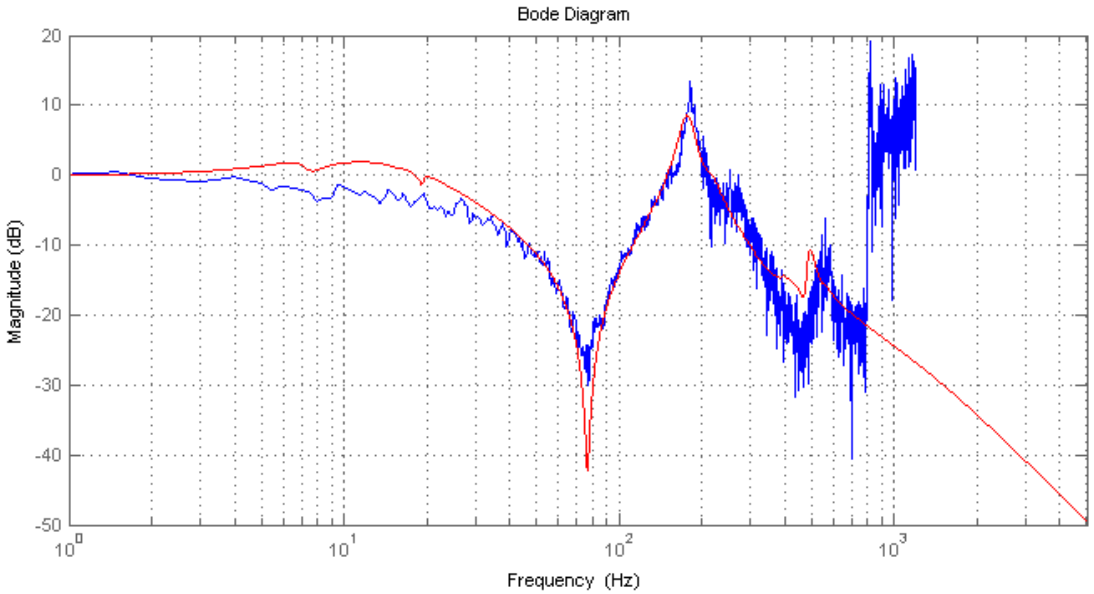

Fig. 12: *Transfer functions – comparison of measurement and calculations with correct parameters (coupling R+W BK2 used, table near PMSM)*

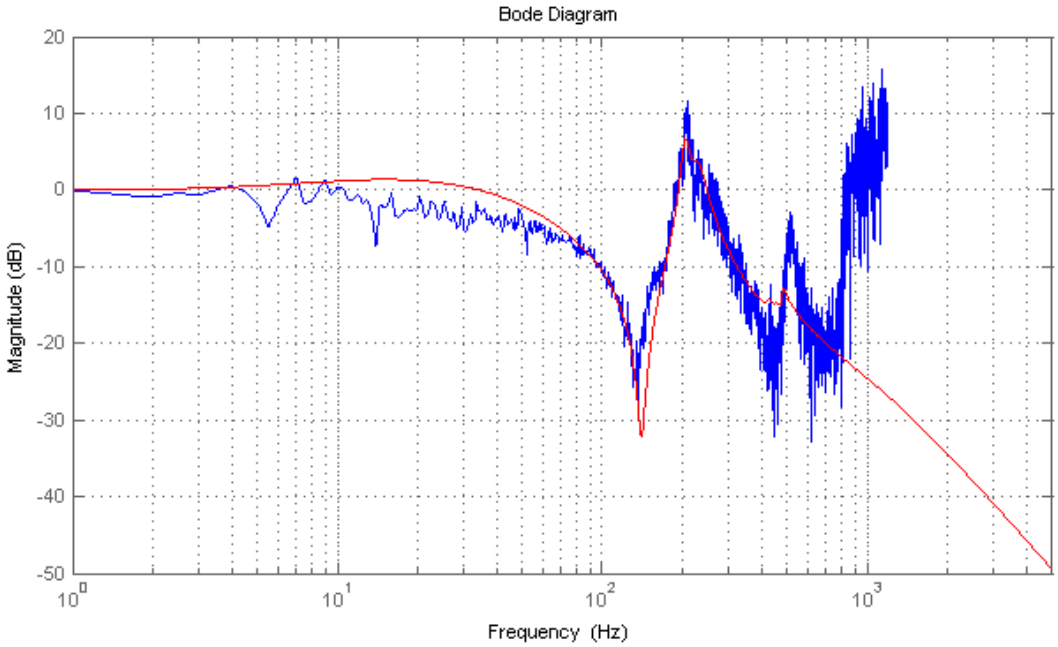

Fig. 13: *Transfer functions – comparison of measurement and calculations with correct parameters (coupling MAYR SMARTFLEX used, table near PMSM)*

The figures 12, 13 and 14 show comparison of the measurements and calculations, each in different conditions. In all three figures blue curve is the measured transfer function of speed control and red curve is the calculated one. All calculated transfer functions have some eigen modes damped to respect structural damping of the sand filling and rubber insulators. In all three figures the measured and calculated functions are very similar. This was the objective of the verification and the parameters of FEM model can be considered correct. In common drives, eigen frequencies are damped by speed control regulator up to about 500 Hz but in my measurements even eigen frequency 200 Hz isn't damped. This is because the input A/D

converter has sampling frequency 1000 Hz which degrades the whole regulation. Due to this fact and some other properties of the measurement equipment, accurate measurements can by obtained only up to 800 Hz. Higher values are highly in error and irrelevant.
Transfer functions in the figure 12 were obtained when using the coupling R+W BK2, the table with additional weight near PMSM. The functions in the figure 13 were obtained when using the coupling MAYR SMARTFLEX, the table without additional weight near PMSM. Different values of the table weight and coupling stiffness result into shifts of eigen and antiresonant frequencies around 100 Hz in the figures 12 and 13. In the figure 13 it is also apparent that the lighter table can't excite vibration of the bed in low frequencies. In the figure 14 the transfer functions are obtained when using the coupling MAYR SMARTFLEX too, but table with additional weight at the far end of the screw (about 1 meter from PMSM – the ball screw is the shorter one). Some shifts are also visible in these functions. Parameters of all used, measured and in-FEM-model-included parts are shown in the table 2. All values are final after the verification.

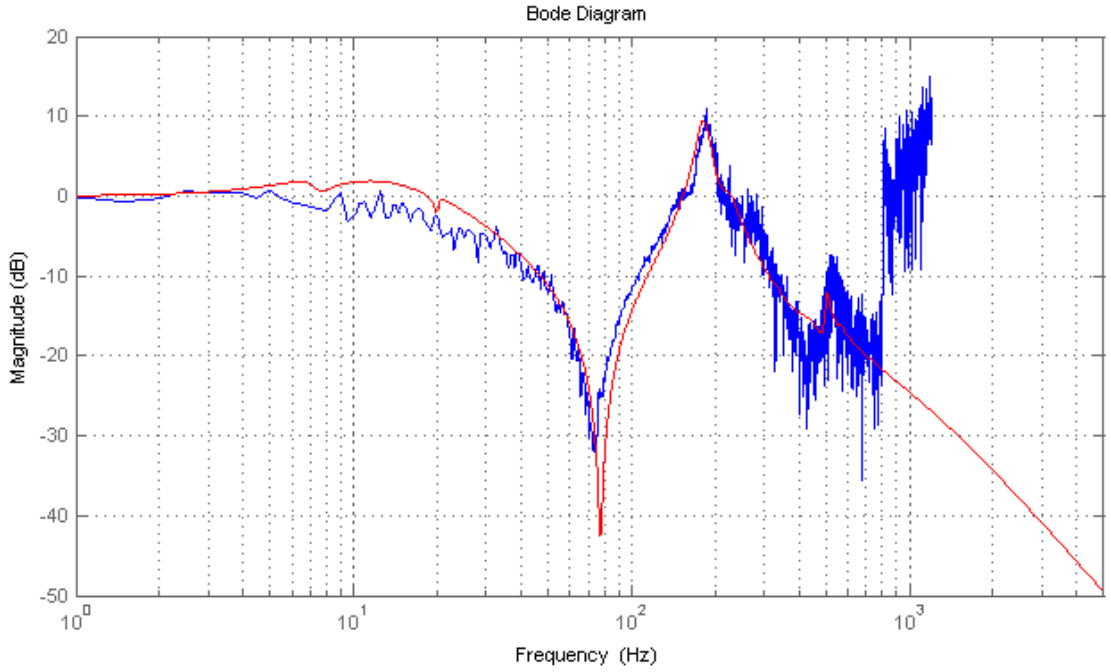

Fig. 14: *Transfer functions – comparison of measurement and calculations with correct parameters (coupling MAYR SMARTFLEX used, table far from PMSM)*

Table 2. *– Parameters of used parts.*

	Type	Parameters
PMSM	BAUMULLER DS56L	$J_m = 1.57 \cdot 10^{-3} kg \cdot m^{-2}$
Coupling	MAYR ROBA ES	$J_c = 5 \cdot 10^{-5} kg \cdot m^{-2}$ $k_{Tc} = 900 Nm \cdot rad^{-1}$
	R+W BK2	$J_c = 7 \cdot 10^{-5} kg \cdot m^{-2}$ $k_{Tc} = 3600 Nm \cdot rad^{-1}$
	MAYR SMARTFLEX	$J_c = 9 \cdot 10^{-5} kg \cdot m^{-2}$ $k_{Tc} = 3200 Nm \cdot rad^{-1}$
Bearing	ZARN 2557 LTNA	$k_{AB} = 1900 \cdot 10^{-6} N \cdot m^{-1}$
Ball nut	KSK 32x32 APQR	$k_N = 300 \cdot 10^{-6} N \cdot m^{-1}$
Table	With additional weight	$m_T = 80 kg$
	Without additional weight	$m_T = 220 kg$

5. Conclusion

Additional simulations and measurements on the 4-mass testing bed were performed. The results of these simulations and measurements show that a significant increase of regulation parameters can be achieved by the usage of 2 PMSMs on one feed axis. CAD and FEM models of the modified testing bed STD-3 (which is more similar to the real machine tool) were created. Measurements on original STD-3 were performed and the results of these measurements were used for verification of the parts parameters. STD-3 is ready for the assembly according to CAD model as soon as it is free of other experiments and teaching lectures.

List of symbols

G_{PI}	speed regulator transfer function	$[A \cdot s \cdot rad^{-1}]$
G_F	current regulator transfer function	$[1]$
K_V	proportional gain of position regulator	$[s^{-1}]$
v_{soll}	desired speed	$[rad \cdot s^{-1}]$
s	parameter of Laplace transform	$[s^{-1}]$
j	complex unit	$[1]$
ω	angular frequency	$[s^{-1}]$
G_{ij}	transfer function of mechanics	$[1]$
M	mass matrix	$[kg]$, $[kg \cdot m^{-2}]$
m_i	weight (moment of inertia) of i-th mass (general – element of M)	$[kg]$, $[kg \cdot m^{-2}]$
B	friction matrix	$[kg \cdot s^{-1}]$, $[kg \cdot m^{-2} \cdot s^{-1}]$
K	rigidity matrix	$[kg \cdot s^{-2}]$, $[kg \cdot m^{-2} \cdot s^{-2}]$
k_i	rigidity of i-th spring(general – element of K)	$[kg \cdot s^{-2}]$, $[kg \cdot m^{-2} \cdot s^{-2}]$
y	position vector	$[m]$, $[rad]$
y_i	position of i-th mass (general – element of y)	$[m]$, $[rad]$
φ_{iact}	actual rotational position of i-th mass	$[rad]$
φ_{isoll}	desired rotational position of i-th mass	$[rad]$
f	force vector	$[N]$, $[Nm]$
M_{Ki}	torque on i-th mass	$[Nm]$
G	transfer function matrix	$[s^{-1}]$
K_P	proportional gain of speed regulator	$[A \cdot s \cdot rad^{-1}]$
T_N	time constant of speed regulator	$[s]$
J_m	moment of inertia of PMSM	$[kg \cdot m^{-2}]$
J_c	moment of inertia of coupling	$[kg \cdot m^{-2}]$
k_{Tc}	rotational rigidity of coupling	$[Nm \cdot rad^{-1}]$
k_{AB}	axial rigidity of axial bearing	$[N \cdot m^{-1}]$
k_N	axial rigidity of axial bearing	$[N \cdot m^{-1}]$
m_T	weight of sliding table	$[kg]$

References

[1] SICHEN, Fang, BO, Zhou, YING, Liu. Design and realization of dual redundancy PMSM electrical drive systems. Industrial Electronics and Applications, 2009. ICIEA 2009. 4th IEEE Conference on (978-1-4244-2799-4) 25-27 May 2009. p. 1985-1989

[2] GOMAND, Julien, BEAREE, Richard, KESTELYN, Xavier, BARRE, Pierre-Jean. Physical dynamic modelling and systematic control structure design of a double linear drive moving gantry stage industrial robot. European conference on pover electronics and applications, 2007, p. 1231-1239

[3] PARK, Heung-Keun, KIM, Sung-Su, PARK, Jin-Moo, CHO, Tae-Yeon, HONG, Daehie. Dynamics of dual-drive servo mechanism. IEEE International Symposium on Industrial Electronics 2001, ISIE 2001, p. 1996-2000.

[4] CHU, Baeksuk, KIM, Sungsoo, HONG, Daehie, PARK, Heung-Keun, PARK, Jin-Moo. Optimal cross-coupled synchronizing control of dual-drive gantry system for a SMD assembly machine. JSME International Journal, Series C – Mechanical Systems, Machine Elements and Manufacturing, vol. 47, 2004, p. 939-945.

[5] KITAMURA MACHINERY CO LTD. Drive unit for NC machine tool. Kitamura Kosaku, Yamada Shigeru (inventors). Japan JP2001259953 (A). 2001-09-25.

[6] SOUČEK, Pavel, NOVOTNÝ, Lukáš, RYBÁŘ, Pavel. Výzkum regulace pohonů v posuvech NC strojů – Část A. Paralelní chod dvou motorů se společným odměřováním polohy. Praha: VCSVTT, 2009. V-09-061.